Proceedings of the Pakistan Academy of Sciences: A Physical and Computational Sciences 63(3): ------- (2026)
Copyright © Pakistan Academy of Sciences
ISSN (Print): 2518-4245; ISSN (Online): 2518-4253
http://doi.org/10.53560/PPASA(63-3)719

Pakistan Academy of Sciences

Research Article

Improving the Accuracy and Reliability of Plasma Temperature Determination in Laser–Induced Breakdown Spectroscopy

Saba Munir[1], Nasar Ahmed[1], Amir Fayyaz[2,3,*], Usman Liaqat[4], Rinda Hedwig[5], Rizwan Ahmed[2], and Muhammad Aslam Baig[2,3]

[1]Department of Physics, King Abdullah Campus, University of Azad Jammu and Kashmir, Muzaffarabad, 13100, Pakistan
[2]National Centre for Physics, Quaid-i-Azam University Campus, Islamabad, Pakistan
[3]Department of Physics, Quaid-i-Azam University, Islamabad 45320, Pakistan
[4]School of Chemical and Materials Engineering, National University of Science and Technology (NUST), Islamabad, Pakistan
[5]Computer Engineering Department, Bina Nusantara University, Jakarta 11480, Indonesia

ACCEPTED MANUSCRIPT

Abstract: Laser-induced breakdown spectroscopy (LIBS) is a promising analytical technique for rapid, simultaneous multielement analysis. However, shot-to-shot plasma fluctuations and measurement uncertainties can affect the accuracy and reliability of plasma excitation temperature determination. The present work proposes a statistical uncertainty–analysis framework for improving the reliability of plasma excitation temperature determination using the Boltzmann plot method. A LIBS analysis has been carried out using different CoCrCuNi–Pb alloy samples with varied chemical composition of major and minor elements. Pb(I) emission lines are of interest, with negligible spectral interferences and covering a wide range of upper excitation energies. For each sample, 50 LIBS spectra were recorded, and each spectrum was the average of 15 single shots. Plasma temperature is estimated using the net intensity of the selected Pb emission lines in the Boltzmann plot method. The statistical analysis of 50 temperatures was carried out to evaluate the mean value of plasma excitation temperature, standard deviation (*SD*), relative standard deviation (*RSD*), and combined uncertainty. The estimated plasma excitation temperatures using the proposed procedure were in the range from 11000 K to 13000 K with R^2: 0.916 to 0.988; whereas, the *SD* and *RSD* values were in the range of 257–300 K and 2.3–2.4%, respectively. In addition, the Boltzmann plots were constructed using the averaged intensities for each sample, yielding analogous plasma excitation temperatures of 11300–13800 K with R^2: 0.897 to 0.971. The use of the average net intensity in the Boltzmann equation for plasma estimation provides LIBS spectral data with acceptable precision and linearity. Interestingly, both temperature calculations with raw net intensity and with average intensity are in good agreement. Therefore, the study suggests an accurate and reliable determination of plasma excitation temperature using the present in-house developed LIBS setup, which supports the reliability and repeatability of the plasma temperature determination under the experimental conditions used in this study.

Keywords: Laser-induced Breakdown Spectroscopy, Plasma Excitation Temperature, Boltzmann Plot, Uncertainty Analysis, Repeatability, CoCrCuNi–Pb Alloys.

1. INTRODUCTION

Laser-induced breakdown spectroscopy (LIBS) is one of the promising analytical techniques for rapid and reliable elemental analysis due to its inherent advantages, such as minimal sample preparation, real-time response, simultaneous detection of multiple elements, and versatility for solid, liquid,

Received: July 2026; Revised: August 2026; Accepted: September 2026
* Corresponding Author: Amir Fayyaz <amirfayyaz@phys.qau.edu.pk>

and gaseous materials [1]. In LIBS, a high–intensity laser beam is focused on the surface of the target material to form a microplasma consisting of electrons, ions, atoms, and molecules generated as a consequence of laser–induced ablation. The expanding and cooling plasma emits light from electronic transitions of excited atoms and ions, from which characteristic emission spectra are recorded for qualitative and quantitative analysis [2]. Due to its minimally destructive nature, high temporal and spatial resolution, rapid analysis, and ability to perform both in–situ and remote measurements, LIBS has been widely used for metallurgy, environmental monitoring, geochemical prospecting, industrial control, cultural heritage studies, biomedical research, and materials science [3, 4].

Among a variety of materials studied by LIBS, multi–component metallic alloys are considered a class of materials whose physical, chemical, electrical, and mechanical properties are sensitive to changes in their elemental composition and microstructure [5]. CoCrCuNi–Pb high-entropy alloys are used to produce parts for aircraft engines, machine–building, tool engineering, electrical engineering, and friction–reducing mechanisms. They are selected for these applications because they combine high mechanical strength and hardness with high resistance to thermal shock, chemical attack, and excellent machinability, plasticity, and electrical conductivity [6]. Cobalt and nickel improve the alloy's stability at elevated temperatures, chromium protects against oxidation and corrosion, copper enhances electrical and thermal conductivity, and lead improves machinability and reduces friction. Therefore, there is a continuous demand to characterize the elemental composition of CoCrCuNi–Pb alloys for quality control and process optimization purposes.

The analytical performance of LIBS is largely determined by the physicochemical properties of laser–induced plasma. Different parameters, namely, excitation temperature, electron density, and chemical composition, determine the mechanisms of atomic excitation and ionization processes occurring in plasma and, thus, affect the accuracy of analytical LIBS results [7, 8]. In particular, the excitation temperature of LIBS plasma impacts the population densities of excited states of atoms and ions in accordance with the Boltzmann distribution function [9]. Therefore, an accurate measurement of the temperature parameter is critical for investigating the temporal evolution of the plasma, validating the local thermodynamic equilibrium (LTE) condition, implementing a calibration–free LIBS approach, and obtaining accurate and reliable analytical quantifications [10-12]. Various optical emission spectroscopy methods have been developed for temperature measurements, including the two-line intensity method, the line–to–continuum method, the Saha–Boltzmann plot method, and the Boltzmann plot method. Among these techniques, the Boltzmann plot method is the most common one due to the simplicity of its implementation and theoretical formulation, as well as the possibility of using it under conditions of optical thinness and LTE. According to this method, the natural logarithm of the intensity of selected emission lines is linearly correlated with their excitation energy, and the slope of the linear regression is inversely related to the plasma excitation temperature. However, various factors, including the choice of emission lines, detector characteristics, spectral resolution, signal–to–noise ratio, self–absorption effects, spatial inhomogeneity of the plasma, and shot–to–shot variability of plasma formation, may affect the accuracy of plasma temperature measurements. Therefore, even for a LIBS measurement performed under identical experimental conditions, the emission line intensities may vary drastically for different laser shots, which introduces uncertainty in the determination of plasma temperatures.

Recently, Bousquet *et al.* [13] evaluated the uncertainty and reliability of plasma excitation temperature estimated using the Boltzmann plot method, considering the effects of signal–to–noise ratio, spatial and temporal integration, and measurement sensitivity. John *et al.* [14] studied uncertainties in conventional calibration–free LIBS by employing a multi–element Saha–Boltzmann plot approach, which reduces the influence of transition-probability variations, statistical fluctuations, and self–absorption. The presented method improves the precision and reliability of quantitative elemental analysis compared with conventional CF–LIBS. Gornushkin *et al.* [15] investigated the uncertainty introduced by spatial and temporal non-uniformity of laser-induced plasma in Boltzmann plot–based temperature and concentration measurements. Plasma modeling

ACCEPTED MANUSCRIPT

shows that such non–homogeneity can limit the accuracy of temperature estimation and lead to significant errors in the determination of minor and trace elemental concentrations. Therefore, uncertainty analysis of temperature derived from Boltzmann plots is critical because plasma non–uniformity, signal–to–noise ratio, line selection, and measurement fluctuations can significantly affect the estimated temperature. Reliable uncertainty quantification is therefore essential to establish the precision, accuracy, and physical validity of the measured plasma temperature and subsequent elemental concentrations.

In this study, seven CoCrCuNi–Pb alloy samples were investigated using two approaches for plasma excitation temperature determination. In the proposed approach, a separate Boltzmann plot was constructed for each of 50 independently acquired LIBS measurements, each measurement consisting of an average of 15 laser shots. The resulting 50 temperature values were statistically analyzed to determine the mean temperature, standard deviation, relative standard deviation, and uncertainty. For comparison, a conventional intensity–averaging approach was employed in which the 50 spectra were first averaged to obtain a single representative spectrum and subsequently used to construct one Boltzmann plot.

2. MATERIALS AND METHODS

2.1. Sample Preparation

Seven alloy samples containing Co, Cr, Cu, Ni, and Pb were prepared for the LIBS experiment to determine the reliability of the plasma excitation temperature. High-purity elemental powders with purities of 99.5–99.9% were used to prepare the alloy samples. To reduce the effect of impurities on the plasma properties, the elements were taken in the amounts indicated in Table 1 and weighed on an analytical balance with an accuracy of ±0.1 mg. The powders were mixed in a porcelain mortar to obtain homogeneous mixtures for further pellet formation. A hydraulic press was used to form the pellets by static compression at a pressure of 50 MPa for 20 min. The pellets thus obtained had a diameter of about 25 mm, a thickness of 6 mm, and a mass of 2 g. In addition, good quality flat pellets were obtained, which provide reliable LIBS emission results when exposed to laser pulses. To remove any trace of organic contaminants from the surface of the pellets, they were washed with ethanol. To find out how much the alloy composition affects the accuracy of the measurement and the value of plasma excitation temperature, seven Pb–based alloy samples were prepared using the aforementioned procedure. Sample (S1) was initially used to identify and select eight suitable Pb emission lines for the Boltzmann–plot analysis based on their spectral intensity, isolation from interfering lines, and relevance for temperature determination. After selection, the same eight Pb emission lines were consistently used for all samples (S1–S7) to determine the plasma excitation temperature under identical experimental conditions. The alloy samples (S2–S7) were then used to evaluate the reproducibility and reliability of the plasma–temperature measurements and to assess the uncertainty of the mean plasma temperature by

ACCEPTED MANUSCRIPT

Table 1. Concentrations of Co, Cr, Cu, Ni, and Pb in pelletized alloy samples (wt.%).

	Element Chemical Composition (wt.%)				
Sample	**Cobalt (Co)**	**Chromium (Cr)**	**Copper (Cu)**	**Nickel (Ni)**	**Lead (Pb)**
S1	18.10	15.00	19.30	18.10	29.50
S2	17.60	14.60	18.80	17.60	31.40
S3	17.10	14.20	18.30	17.10	33.30
S4	16.60	13.80	17.80	16.60	35.20
S5	16.18	13.47	17.39	15.67	37.29
S6	15.60	13.00	16.80	15.60	39.00
S7	15.09	12.58	16.28	15.09	40.96

comparing the estimated temperatures and their corresponding *RSD* values.

2.2. LIBS Experimental Setup

The configuration of the LIBS experimental system used in the present study is shown in Figure 1. A Q-switched Nd:YAG laser with a wavelength of 532 nm was used as an excitation source, while the laser pulses with a duration of about 5 ns could provide up to 400 mJ of maximum energy per pulse [16-18]. A plano-convex quartz lens with a focal length of 150 mm was used to focus the laser beam onto the surface of the established Pb-based alloy sample. However, to stabilize the plasma parameters and reduce the inter-shot variability, a pulse energy of 80 ± 0.25 mJ was used during the experiments. In this case, a fiber-optic cable was placed at a 90° angle to the surface of the sample to collect the maximum amount of the plasma emission, while an optical fiber with a 600 µm core diameter was used to transmit the light. A detection system was designed based on an Avantes spectrometer with a built-in CCD array, covering the spectral range from 200 to 970 nm. The aforesaid acquisition system is capable of simultaneously analyzing the emission lines of Co, Cr, Cu, Ni, and Pb in the alloy samples. A digital delay interval generator was used to control the timing of the start of the detection system. In this regard, the temporal resolution of the plasma emission was optimized by adjusting the delay and gate width of the CCD detector. The continuum emission from the recorded spectra was removed using a baseline-subtraction procedure in the Avantes software during the recording of the emission spectra, and only feature spectra were recorded and used for further analysis.

The LIBS experiments were performed under optimized and the same experimental conditions for all samples to ensure reproducibility and consistency of results. For each LIBS measurement, the sample surface was moved to a new position by the motorized sample stage to avoid crater overlapping and multiple ablations at the same spot on the sample surface. For each sample, 50 representative emission spectra under the same conditions were recorded. Each spectrum was an average of 15 single–shot spectra to remove the random errors that could occur due to the LIBS spectral shot–to–shot instability. Thus, 50 LIBS spectra per alloy sample were acquired and processed to perform further analysis. The emission lines of Co, Cr, Cu, Ni, and Pb were identified based on the data from the NIST atomic spectra database [19] to build the characteristic emission spectra. By using the averaged spectra of CoCrCuNi–Pb alloy samples, the best transition lines of Pb(I) with high intensity, good–to–excellent signal–to–background ratios, and moderate–to–good spectral resolution were selected for the temperature analysis. To calculate the statistical variation of 50 measurements of the plasma temperature for each sample, the mean plasma temperature, standard deviation (*SD*), relative standard deviation (*RSD*), and combined uncertainty were computed. The calculated statistical errors were used to compare the LIBS performance for the 7 analyzed samples of CoCrCuNi–Pb alloys.

ACCEPTED MANUSCRIPT

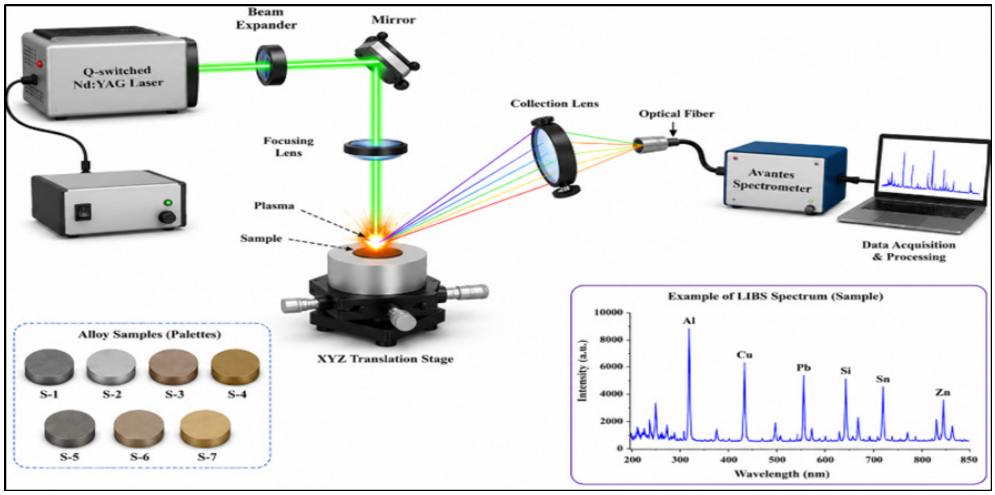

Fig. 1. LIBS Experimental setup contains an Nd:YAG laser system, optical components, Avantes spectrometer, sample stage, and alloy pellets.

2.3. Analytical Plasma Characterization

The plasma excitation temperature was evaluated using the Boltzmann plot method, which is one of the most common methods for determining plasma temperatures under the assumption of local thermodynamic equilibrium (LTE) [20]. LTE validation is important for the consistency of the spectroscopic analysis, as the assumption of LTE provides a basis for relating the measured spectral characteristics to the thermodynamic properties of the investigated optical plasma. The validity of LTE is generally assessed using appropriate plasma parameters and established equilibrium criteria [21]. In the present study, the obtained experimental conditions satisfy the relevant considerations for LTE, supporting the reliability of the derived spectroscopic parameters. LTE allows the population of the excited atomic energy levels to be described by the Boltzmann distribution, and the plasma excitation temperature can be calculated from the slopes of the natural logarithm of the emission intensities of the selected transitions.

In order to use the Boltzmann plot method, certain requirements should be met. Firstly, the selected emission lines should originate from an optically thin plasma. Secondly, the transition probability, statistical weight, wavelength, and upper energy level of the chosen spectral lines should be known. The optically thin condition of the plasma was evaluated using the line–pair intensity-ratio method. Two emission lines originating from the same species and having comparable spectroscopic characteristics were considered, and their measured intensity ratio was compared with the corresponding theoretical ratio expected in the absence of self–absorption. A close agreement between the measured and theoretical intensity ratios indicates that the selected transitions are not significantly affected by self–absorption. The line–pair analysis showed no significant deviation from the expected intensity ratio, suggesting that self–absorption was negligible under the experimental conditions. Therefore, the selected Pb emission lines were considered sufficiently optically thin and suitable for reliable Boltzmann-plot plasma-temperature determination. In this work, the atomic data of the selected Pb(I) transitions were retrieved from the NIST atomic spectral database [19]. Eight Pb(I) emission lines, which met the criteria of high emission intensity, low spectral interference, wide excitation–energy range, and known spectroscopic parameters, were used to calculate the excitation temperature of the plasma using the Boltzmann plot method. The use of multiple Pb(I) transitions for the calculation of the excitation temperature reduces the random error associated with the measurement of the emission intensity of a particular spectral line. The excitation temperature of the plasma was calculated using the following Boltzmann equation [22, 23].

$$ln\left(\frac{I_{ij}\lambda_{ij}}{hcA_{ij}g_i}\right) = -\frac{E_i}{k_B T_e} + \ln\left(\frac{N_e}{P(T_e)}\right) \qquad (1)$$

where I_{ij} is the measured emission intensity, λ_{ij} is the wavelength of the spectral transition, A_{ij} is the transition probability, g_i is the statistical weight of the upper energy level, E_i is the corresponding excitation energy, h is Planck's constant, c is the speed of light, k_B is the Boltzmann constant, and T_e is the plasma excitation temperature. In this contribution, the Boltzmann plot was constructed by taking the natural logarithm of the left-hand side of Equation (1) versus the corresponding upper excitation energies of the chosen Pb(I) emission lines. Then the linear regression method was applied to the set of experimental points, and the plasma excitation temperature was evaluated from the slope of the best-fit straight line according to the following equation [22, 23].

$$T_e = -\frac{1}{k_B \times slope} \qquad (2)$$

For each alloy sample, 50 independent Boltzmann plots were calculated using the 50 averaged LIBS spectra, each of which was obtained by averaging the emission intensities of 15 laser shots. Thus, 50 independent plasma excitation temperatures were calculated for each sample. The temperature data obtained were then used to calculate the mean plasma temperature, standard deviation (*SD*), relative standard deviation (*RSD*), and combined uncertainty, which allowed us to assess the stability and reproducibility of the LIBS measurements. In contrast to the conventional approach, in which the plasma temperature is estimated from one averaged Boltzmann plot, we therefore constructed, from the intensities averaged over 15 laser shots, a temperature value for 50 independent measurements, which provides a better precision estimate. Note that each measurement was acquired from a fresh, non-overlapping position on the sample surface, and therefore the 50 averaged spectra were treated as independent measurements.

ACCEPTED MANUSCRIPT

2.4. Uncertainty Analysis

In order to estimate the repeatability of the results and the reliability of the measured values of the plasma excitation temperature, a statistical uncertainty analysis was carried out for the plasma temperatures determined by 50 independent LIBS measurements for each analyzed alloy sample. Each measurement used the average of 15 laser shots under the same conditions. This reduced random noise while keeping the true signal from the laser plasma. Plasma excitation temperatures were calculated from the 50 LIBS spectra, and then the average temperature, standard deviation (*SD*), and relative standard deviation (*RSD*) were evaluated to describe their statistical distribution. The standard deviation [24] was calculated using the following relation.

$$SD = \sqrt{\sum_{i=1}^{N} \frac{(T_i - T)^2}{N-1}} \quad (3)$$

where T_i is the plasma excitation temperature determined from each LIBS emission spectrum, T is the mean plasma excitation temperature, and N is the number of independent measurements (N = 50). To estimate the repeatability of the plasma temperature measurements independent of their absolute value, the relative standard deviation (*RSD*) was calculated using the following relation [25].

$$RSD(\%) = \frac{SD}{T} \times 100 \quad (4)$$

where *SD* is the standard deviation, and T is the corresponding mean plasma temperature. To further quantify the collective uncertainty associated with the plasma excitation temperature measurements, the combined uncertainty (U_c) was estimated. The combined standard uncertainty (U_c) of the plasma excitation temperature was estimated by considering the relevant independent uncertainty contributions expressed in terms of their relative standard deviations (*RSDs*).

$$U_c = \mathrm{T}\sqrt{\sum_{i=1}^{n} \left(\frac{RSD_i}{100}\right)^2} \quad (5)$$

where RSD_i is the relative standard deviation associated with each independent uncertainty component, and T is the mean plasma excitation temperature. This value accounted for the overall precision of the measurements, related to shot–to–shot plasma fluctuations, and was represented as error bars in the plots. Using error bars allowed an estimate of the confidence intervals for the measured quantities and, therefore, provided a reliable comparison of the results for different alloy samples. Unlike the previously described approach, which is used conventionally in such cases, where calculation of one Boltzmann plot based on averaged intensities leads to one plasma temperature value, the current method determines the temperature values independently for 50 spectra averaged for each alloy sample. Therefore, the statistical distribution of the obtained values can be used to estimate the spread and uncertainty of the measurements, which is especially important for LIBS, which is known to have relatively large fluctuations due to the nature of the LIBS measurement procedure. The uncertainty–analysis procedure used in this study is applied to the set of 7 pelletized CoCrCuNi–Pb alloy samples; the resulting average plasma temperatures, standard deviations, relative standard deviations, and combined uncertainty estimates are used to assess the repeatability of measurements.

3. RESULTS AND DISCUSSION

3.1. LIBS Emission Spectrum

The representative LIBS emission spectra of the fabricated CoCrCuNi–Pb alloy samples (S1–S7) between 215 and 900 nm are presented in Figure 2. For each alloy sample, 50 independent LIBS measurements were carried out under the same experimental conditions using a Q-switched Nd:YAG laser emitting light at 532 nm with a fixed pulse energy of 80 ± 0.25 mJ. For each measurement, the single averaged LIBS spectrum was acquired from 15 consecutive laser pulses. The presented LIBS spectra are typical for all studied alloys and serve for further discussion of analytical results and plasma diagnostics. Figure 2 reveals that the spectra of alloy samples under investigation have a similar trend within the whole range of wavelengths. The similarity of the spectra is expected because all CoCrCuNi–Pb alloy samples contain the same five constituent elements, although their relative compositions differ. The similarity in spectral profiles suggests that the ablation and plasma generation conditions were reasonably consistent across the measurements. However, Figure 2 shows that some spectral lines have different intensities for the alloys under investigation. Apart from random noise, which

ACCEPTED MANUSCRIPT

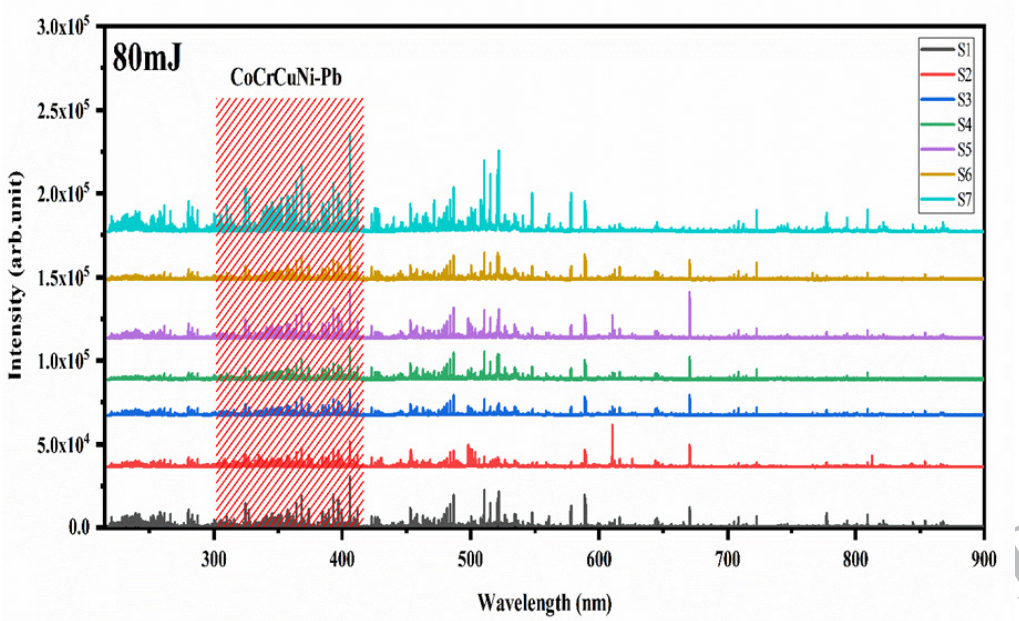

Fig. 2. Representative LIBS emission spectra of the seven prepared CoCrCuNi–Pb alloy samples (S1–S7) recorded under identical experimental conditions.

may have originated from the instability of LIBS measurement conditions, different intensities of emission lines could be associated with variations in elemental composition of the prepared alloys. On the one hand, the discussed LIBS spectral characteristics of CoCrCuNi–Pb alloys indicate the possibility of differentiating between the studied materials. On the other hand, the similar overall trends of LIBS spectra prove the stability of the LIBS signal during the experiments. The recorded broadband LIBS spectra contain a large number of atomic and ionic emission lines coming from the ablated material. It should be noted that the analysis of the whole set of spectral lines is not always informative due to significant overlapping of particular spectral lines. To identify distinct spectral features of CoCrCuNi–Pb alloys, the broadband spectra between 215 and 900 nm were separated into several spectral ranges. The division of the LIBS spectrum into ranges allows both the intense and weak emission lines to be clearly seen without overlapping each other.

Furthermore, the LIBS emission spectra recorded in air contain several emission lines originating from atmospheric species such as H, N, and O. Because the LIBS measurements in this study were performed in air, the recorded emission spectra were corrected for the underlying plasma continuum emission, which mainly originates from processes such as bremsstrahlung and radiative recombination, before the analysis of emission lines from the alloy constituents. As shown in Figure 2, the corrected (background–subtracted) LIBS spectra still exhibit weak emission features from atmospheric species, which have a negligible influence on the identification and analysis of the characteristic emission lines of the CoCrCuNi–Pb alloys. Therefore, particular attention was given to the emission lines of Co, Cr, Cu, Ni, and Pb for elemental identification and plasma–temperature determination.

The shaded area shown in Figure 2 covers the emission lines of Co(I), Cr(I), Cu(I), Ni(I), and Pb(I) that were selected for the qualitative and quantitative analysis of the alloying elements. These spectral lines were identified using the NIST atomic spectral database [19], and the calculated wavelengths were found to be in good agreement with the reported values for these elements. This allowed determining the contents of the selected alloying elements in all of the studied samples. Since the selected emission lines originate from different elements that demonstrate distinct features in their spectra, each of them is discussed separately in the following section. Furthermore, the information provided allows for discussing the calculation of the excitation temperature of the plasma and the statistical uncertainty of the measured contents of Pb(I), which is one of the selected elements whose emission lines were used in the calculations.

ACCEPTED MANUSCRIPT

Figure 3 provides the selected neutral cobalt Co(I) emission lines detected in the LIBS representative spectrum of the prepared CoCrCuNi–Pb alloy sample (S1). The cobalt emission lines identified in the recorded LIBS spectrum were numerous, although only the most prominent, well-resolved, and isolated transitions are presented for further consideration. In particular, the Co(I) transitions at wavelengths 340.477, 340.871, 341.204, 341.446, 344.880, 345.300, and 350.186 nm were used to illustrate the LIBS characteristics of cobalt in the given CoCrCuNi–Pb alloy sample. All selected transitions were found at wavelengths corresponding to the data reported by NIST [19]. The electronic transition of neutral cobalt ions, Co(I), was classified as $3d^7(^4F)4s \rightarrow 3d^7(^4F)4p$, which is a strong transition for detecting cobalt in the LIBS spectrum.

Among the presented Co (I)emission lines, the two strongest spectral lines at central wavelengths of 345.30 and 350.19 nm were detected, whereas the remaining four spectral lines also demonstrated reasonably high peak intensities and resolution. In particular, the emission lines of Co(I) were observed as isolated spectral lines with high resolution, assisting the evaluation of their peak intensities. Furthermore, the given Co(I) transitions were found to be well-separated from the spectral lines of other elements (Cr, Cu, Ni, and Pb), which is critical for any LIBS analysis. Additionally, it is worth noting that several intense emissions of cobalt were detected within a reasonably small range of wavelengths. As seen in Figure 3, there are several strong, isolated Co(I) emission lines, suggesting the possibility of identifying multiple transitions for plasma diagnostics and cross–verifying the LIBS measurements of cobalt. The Co(I) transitions presented in Figure 3 were not applied for diagnosing the plasma temperature due to the complexity of the Co spectra. Nevertheless, the general ability of the given LIBS system to produce consistent emission spectra was demonstrated, allowing successful Co(I) detection within each spectrum. Thus, the Co(I) emission lines at 340.477, 340.871, 341.204, 341.446, 344.880, 345.300, 350.186 nm were found to provide adequate spectral features for subsequent LIBS analysis of cobalt in the CoCrCuNi–Pb alloy.

Figure 4 shows the selected neutral chromium Cr(I) emission lines from the LIBS spectrum of the prepared CoCrCuNi–Pb alloy sample. Since there were several chromium emission lines were observed in the obtained LIBS spectrum, only the most prominent ones are presented and discussed. The selected Cr(I) emission lines are centered at 425.441, 427.481, and 428.972 nm. These wavelengths are in good agreement with the reference data retrieved from the NIST atomic spectral database [19]. These spectral lines are commonly observed in LIBS measurements originating from chromium-containing samples. The presented Cr(I) emission lines have a good signal-to-background ratio and therefore can be used for quantitative analyses. Moreover, the chosen Cr(I) emission lines are isolated from other spectral features; hence, their areas can be accurately integrated to estimate the excitation conditions of chromium atoms in the plasma. The LIBS spectrum demonstrates that multiple Cr(I) transitions can be used as indicators of the plasma temperature. The utilization of these spectral lines allows validation of the obtained results of the plasma excitation temperature because of the

ACCEPTED MANUSCRIPT

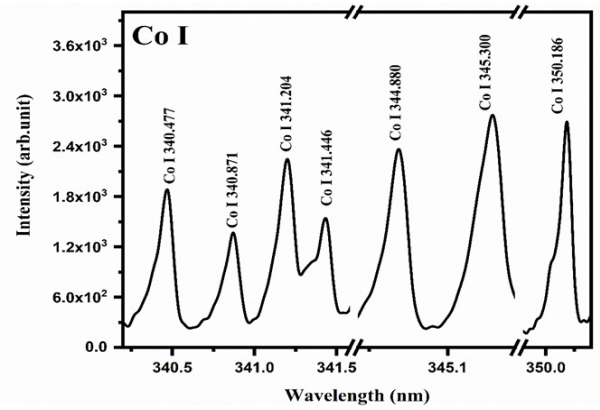

Fig. 3. Selected neutral cobalt Co(I) emission lines in the LIBS spectrum of sample (S1).

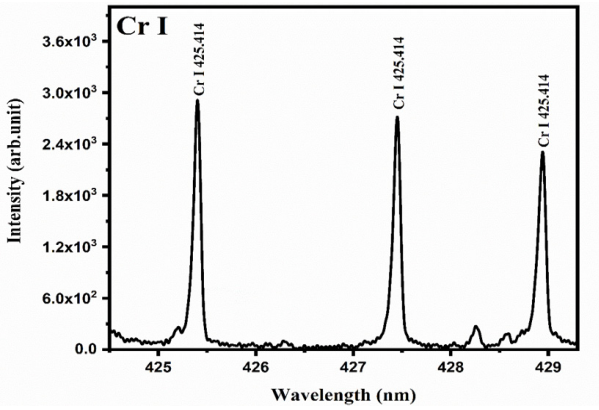

Fig. 4. Selected neutral chromium Cr(I) emission lines in the LIBS spectrum of sample (S1).

observed good agreement between the measured and reference wavelengths of these transitions. Even though the Cr(I) emission lines were not used for temperature calculations, their presence in the LIBS spectrum confirms that chromium atoms were successfully excited in the plasma during the measurement. Therefore, the utilization of these emission lines validates the accuracy of the described LIBS measurements and the reliability of the obtained results.

Figure 5 illustrates the selected neutral copper Cu(I) emission lines detected in the LIBS spectrum of the prepared CoCrCuNi–Pb alloy sample. Out of several observed copper emission lines presented in the spectrum, the two strongest and most intense lines at 324.732 nm and 327.374 nm were chosen for discussion. Both selected copper emission lines have wavelengths in accordance with the data stored in the NIST database [19], thus confirming the correct choice of Cu(I) spectral lines. The observed emission at 324.732 nm and 327.374 nm originates from the $3d^{10}4p \rightarrow 3d^{10}4s$ transition of neutral copper atoms. One can investigate that the strongest Cu(I) emission line is the one at the 324.732 nm peak wavelength. The emission peak at 327.374 nm demonstrates a lower, yet still considerable intensity. Moreover, due to the absence of emission line overlap, one can observe clearly defined 324.732 nm and 327.374 nm peaks with good signal-to-background ratios. Both emission lines are characteristic of intense and efficient excitation of copper atoms within the LIBS plasma.

Figure 6 presents the selected neutral nickel Ni(I) emission lines identified in the LIBS spectrum of the prepared CoCrCuNi–Pb alloy

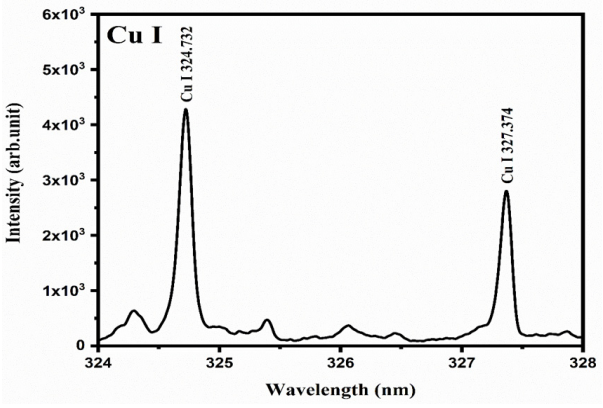

Fig. 5. Selected neutral copper Cu(I) emission lines in the LIBS spectrum of sample (S1).

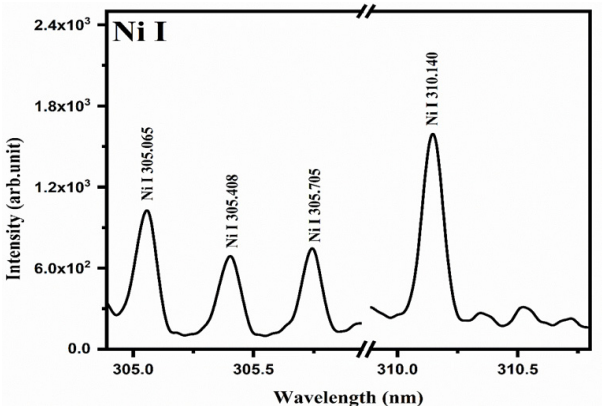

Fig. 6. Selected neutral nickel Ni(I) emission lines in the LIBS spectrum of sample (S1).

sample (S1). From the spectral data of multiple nickel lines present in the spectrum, the emission lines with the highest peak intensities at 305.065, 305.408, 305.705, and 310.140 nm were selected for discussion. All the selected wavelengths are in excellent agreement with the standard data reported by the NIST database [19]. For this reason, the selected emission lines of Ni(I) at 305.065, 305.408, 305.705, and 310.140 nm can be considered characteristic for nickel and frequently used in LIBS analyses of nickel alloys due to their high intensity and required spectral properties. The identified spectral lines originate from the $3d^8(^3F)4s \rightarrow 3d^8(^3F)4p$ electronic transitions in nickel atoms. From the selected nickel emission lines, the highest peak intensity is observed for the Ni(I) 310.140 nm transition. In line, the Ni(I) 305.065, 305.408, and 305.705 nm transitions also possess good intensity and are well resolved with respect to the surrounding spectral lines. The observed good sensitivity and resolution of Ni(I) emission lines allow their efficient use in LIBS for determining the excitation temperature.

Figure 7 shows the selected emission lines of Pb(I) determined from the 7 pelletized CoCrCuNi–Pb alloy samples (S1–S7). The element lead (Pb) was selected as a reference for the plasma diagnostics as it was present in the sample as a base matrix with much higher concentrations than other elements present in the investigated alloy samples. The selected emission lines of Pb(I) exhibited good intensity, high signal–to–background ratio, and measurement repeatability, which are crucial for plasma characterization. All measurements were carried out under the same experimental conditions using a Q-switched Nd:YAG laser with

ACCEPTED MANUSCRIPT

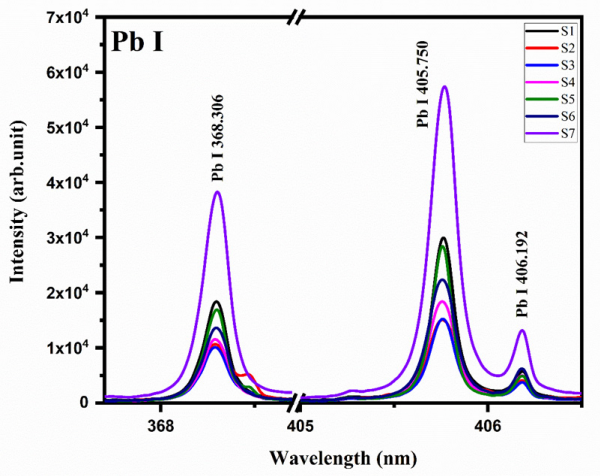

Fig. 7. Selected Pb(I) emission lines of the 7 CoCrCuNi–Pb alloy samples (S1–S7) acquired under identical experimental conditions.

a wavelength of 532 nm, pulse energy of 80 ± 0.25 mJ, 2μs gate delay, 5 ns pulse width, and 10 μs integration time. Each spectrum was an average of 15 single–shot spectra. The experimental conditions and the alloy composition were kept the same throughout the experiment. Therefore, the Pb(I) spectra of the CoCrCuNi–Pb alloy samples (S1 to S7) exhibited similar patterns and line widths. However, variations in the emission intensities were observed due to the variances in the sample chemical compositions. It can be seen that all 7 spectra are consistent with each other, which proves the good reproducibility of the LIBS measurements. The most prominent emission lines of Pb(I) were selected, such as 368.306, 405.750, and 406.192 nm. All three spectral lines were characterized by high emission intensities, good resolution, and absence of spectral interferences. Specifically, the spectral line at 405.750 nm demonstrated the highest intensity for all the analyzed alloy samples, while the line at 368.306 nm is considered the second most intense line in the spectra. The spectral line at 406.192 nm has a lower intensity but a good signal–to–background ratio.

3.2. Plasma Temperature Measurements

The plasma excitation temperature is one of the critical parameters of LIBS plasma, which determines the population distribution of the excited atoms and ions and directly affects the intensity of the spectral lines. In this work, the plasma excitation temperature was evaluated by using the Boltzmann plot method [26, 27]. For this contribution, the neutral lead Pb(I) emission lines were used, having intense, isolated, non–resonant transitions with good upper–level energy spacing, providing accurate linear regression and reliable temperature measurements. In particular, 8 Pb(I) emission lines of interest, such as 247.63, 266.31, 282.31, 287.33, 363.95, 368.306, 405.750, and 406.192 nm, were selected based on their high and unsaturated intensities, good signal–to–background ratios, minimum spectral interferences, and low self–absorption effects. Figure 8(a-g) represents the Boltzmann plots for 7 CoCrCuNi–Pb alloy samples. For each of the plots, the 8 Pb(I) emission lines were taken from the same averaged LIBS spectra over 15 consecutive laser pulses. The error bars represent the standard deviation in the measurements, and the standard deviation is calculated using the 50 measurements for each sample separately.

The representative plots show good linearity between the natural logarithm of the intensity values and the excitation energy of the selected Pb(I) emission lines, suggesting that the measured emission lines can be used for reliable estimation of the plasma excitation temperature. The coefficients of determination (R^2) of the linear fits of the representative plots vary from 0.916 to 0.988. The slope of the representative plots is used to estimate the plasma excitation temperatures, which were found to be 12,700 K for S1 as shown in Figure 8(a), 13,000 K for S2 as displayed in Figure 8(b), 12,400 K for S3 as presented in Figure 8(c), 11,000 K for S4 as revealed in Figure 8(d), 11,000 K for S5 as shown in Figure 8(e), 11,200 K for S6 as displayed in Figure 8(f), and 11,800 K for S7 as exhibited in Figure 8(g). The calculated statistical parameters for 50 measurements of the plasma excitation temperatures for each of the investigated alloys are summarized in Table 2. The results show that for all analyzed alloy samples, the *SD*, *RSD*, and combined uncertainty of all the measurements of the plasma excitation temperatures were low, suggesting that the repeatability and precision of these measurements were excellent. The R^2 values obtained for the representative Boltzmann plots confirm the accuracy of the obtained results and the consistency of using the selected emission lines of Pb(I) for the determination of the plasma excitation temperature. For comparison, the plasma excitation temperature for each alloy was also estimated using the conventional approach, where the emission intensities from 50 independent measurements were

ACCEPTED MANUSCRIPT

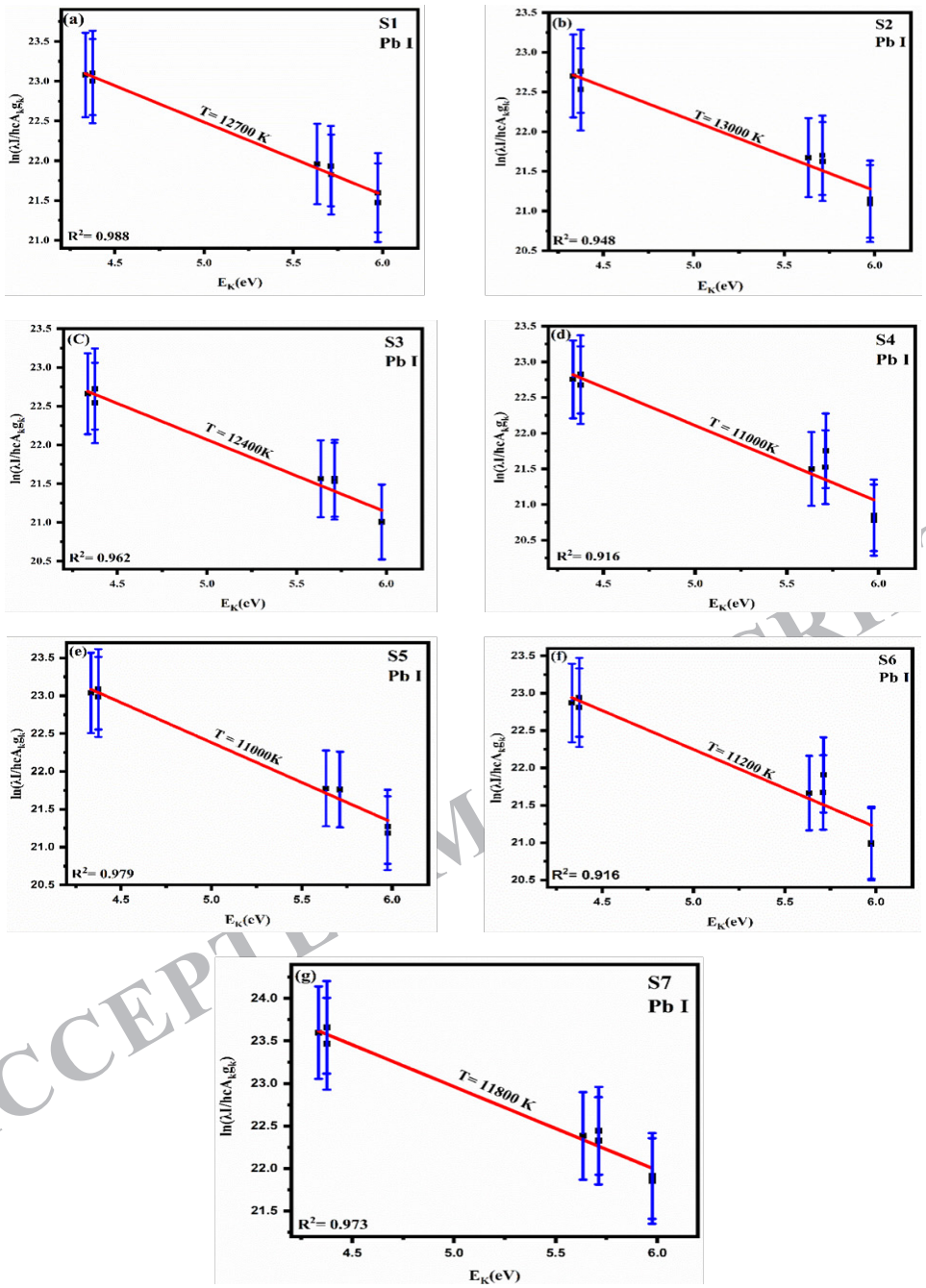

Fig. 8. Representative Boltzmann plots for individual LIBS measurements of the 7 CoCrCuNi–Pb alloy samples: (a) S1, (b) S2, (c) S3, (d) S4, (e) S5, (f) S6, and (g) S7. The temperature is obtained from 50 independent measurements for each sample.

Table 2. Plasma excitation temperatures obtained for the 7 CoCrCuNi–Pb alloy samples.

Sample	Temperature (K)	*SD*	*RSD* (%)	R^2
S1	12,700	300	2.3	0.988
S2	13,000	305	2.3	0.948
S3	12,400	285	2.3	0.962
S4	11,000	268	2.4	0.916
S5	11,000	262	2.3	0.979
S6	11,200	257	2.3	0.916
S7	11,800	270	2.3	0.973

first averaged to construct a single Boltzmann plot, and the slope of this plot was used to calculate the temperature. As expected, the resulting temperatures closely matched the mean values obtained from the 50 individual measurements. However, the conventional approach does not directly preserve the measurement–to–measurement distribution of plasma temperatures and therefore does not provide a straightforward estimate of the variability of the temperature itself.

For comparative study, the seven CoCrCuNi–Pb alloy samples were also analyzed using the conventional intensity–averaged Boltzmann plot method. In this approach, the normalized Pb(I) emission line intensities from 50 independent LIBS measurements for each alloy sample were averaged to create a single representative emission spectrum. The corresponding intensity–averaged Boltzmann plots are shown in Figure 9(a-g), and the plasma excitation temperature for each alloy was determined from the slope of the regression line. The proposed methodology independently determines the plasma excitation temperature for each LIBS measurement prior to statistical analysis, whereas the conventional approach first averages the spectral intensities across measurements. Consequently, the conventional approach yields only a single representative temperature estimate and does not provide information on measurement–to–measurement variability, repeatability, or the associated uncertainty of the temperature determination.

The plasma excitation temperatures calculated from the intensity–averaged Boltzmann plots were ~12,500 K (S1) as shown in Figure 9(a), ~13,800 K (S2) as revealed in Figure 9(b), ~12,800 K (S3) as shown in Figure 9(c), ~11,400 K (S4) as presented in Figure 9(d), ~11,300 K (S5) as demonstrated in Figure 9(e), ~11,600 K (S6) as indicated in Figure 9(f) and ~11,400 K (S7) as appeared in Figure 9(g). All the Boltzmann plots showed good linear trends with excellent determination coefficients (R^2). The obtained temperatures are within the range commonly reported for atmospheric-pressure laser–induced plasmas. Although the spectral averaging process significantly improves the regression linearity by reducing the random spectral noise, the intensities of the selected Pb(I) emission lines revealed significant statistical scattering, which was also manifested by the error bars at corresponding wavelengths. The observed measurement–to–measurement variations in the 15–shot–averaged emission intensities suggest that the LIBS intensities are indeed affected by the random processes involved in the laser-sample interaction. Thus, when performing multiple measurements, the overall random variation in the measured LIBS spectra is reduced due to the spectral averaging procedure. However, it is not possible to completely offset the effect of random processes influencing the shape and the characteristics of the plasma. One of the drawbacks of the conventional approach is that the statistical variations were evaluated based on the intensity values of the selected emission lines rather than the plasma excitation temperatures themselves. Since the 50 independent measurements were combined into one representative spectrum, only one Boltzmann plot was calculated, from which one plasma excitation temperature was determined for each analyzed sample. Consequently, the natural shot–to–shot variations in the LIBS plasma temperatures could not be evaluated. On the contrary, the variability of plasma excitation temperature was found to be relatively small. Although the variability of the 50 averaged intensities revealed valuable information about the measurement stability, it cannot be used as direct evidence of the variability in the plasma excitation temperatures since the variations in the intensities were attributed to various processes rather than temperature changes. The proposed uncertainty–analysis methodology overcomes the limitation of the conventional approach, allowing for preserving the measurement stability information by separately considering plasma excitation temperatures determined from the individual intensity measurements. The 50 temperatures for each sample were then used to estimate the most probable plasma excitation temperature along with the corresponding standard deviation, relative standard deviation, and overall measurement uncertainty. Therefore, the proposed methodology is more physically consistent and transparent as it directly evaluates the measurement uncertainty of the determined plasma temperatures rather than the intensity values. Although both approaches seem to provide comparable measurement stability estimates for the representative intensity–averaged plasma excitation temperatures, the conventional approach lacks physical consistency and transparency, which is critical for accurate LIBS metrology.

ACCEPTED MANUSCRIPT

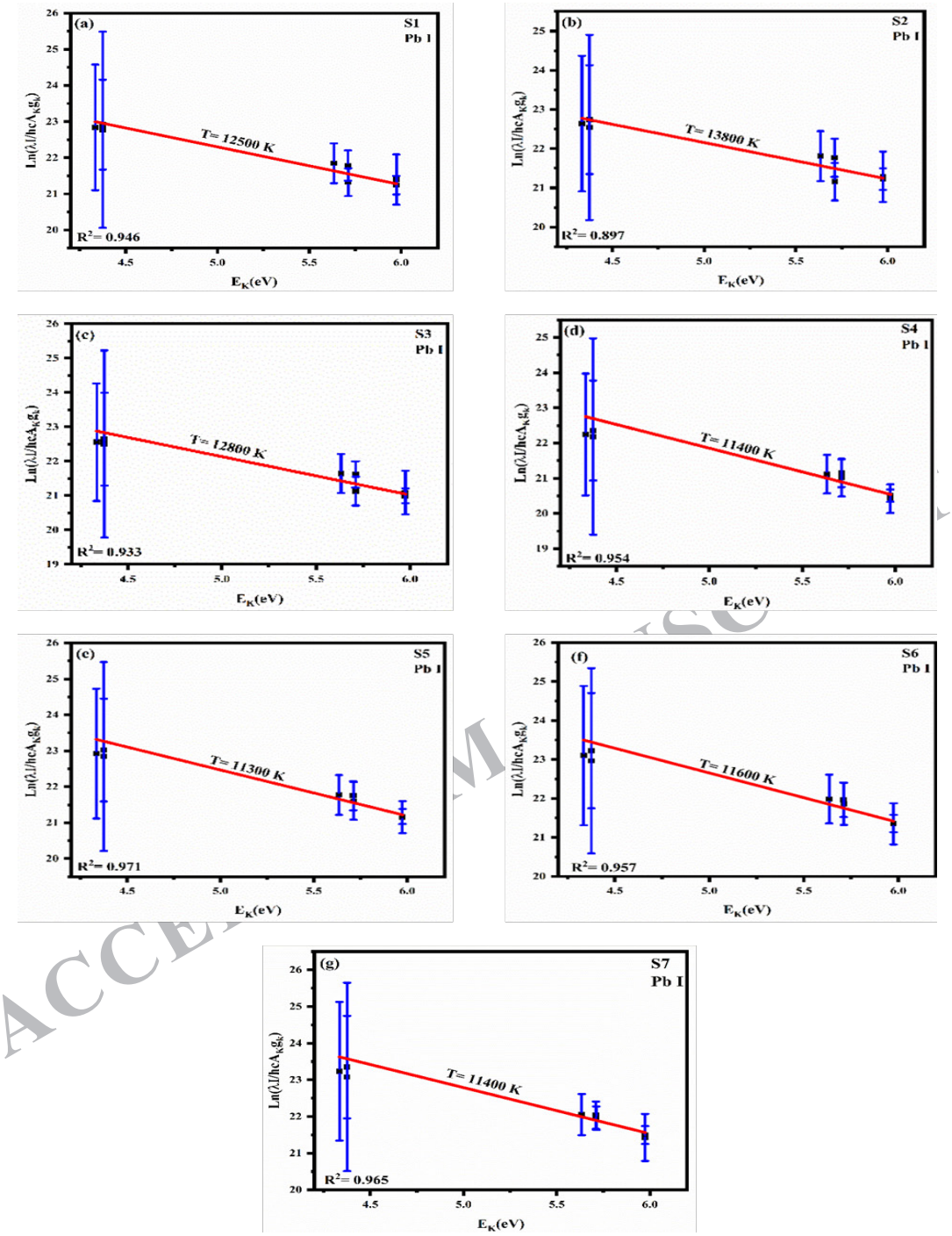

Fig. 9. Conventional intensity–averaged Boltzmann plots of the 7 samples using the 8 selected Pb(I) emission lines: (a) S1, (b) S2, (c) S3, (d) S4, (e) S5, (f) S6, and (g) S7. Each plot was constructed using a representative emission spectrum, which was calculated by averaging the intensities of the individual emission lines from 50 independent measurements (each measurement being an average of the emission intensities from 15 consecutive laser shots).

4. CONCLUSIONS

In brief, a statistical uncertainty–analysis approach was proposed to improve the reliability of plasma excitation temperature determination in LIBS using 7 laboratory–prepared CoCrCuNi–Pb alloy samples. The excitation temperatures of the plasma were determined using the Boltzmann plot method, in which 8 selected Pb(I) emission lines were used to construct temperature plots. Lines were selected based on their high spectral quality, minor spectral interferences, and a considerable range of upper–level excitation energies. A new approach was introduced for a more realistic assessment

of measurement uncertainty by statistically analyzing repeated measurements of plasma excitation temperature instead of calculating an average intensity over multiple laser shots. For this purpose, 50 independent measurements of plasma excitation temperature were made for each alloy sample using averaged LIBS spectra obtained from 15 consecutive laser shots. The estimated plasma temperatures were subjected to statistical analysis to evaluate the mean plasma temperature, standard deviation (*SD*), relative standard deviation (*RSD*), and combined uncertainty. For all samples, the calculated low values of *SD* and *RSD* indicated a high degree of measurement reproducibility, stability of plasma production, and reliability of the estimated plasma excitation temperature. As a result of the comparison between the proposed approach and the conventional intensity–averaged Boltzmann plot method, it was found that both methods are in good agreement. However, while the conventional approach calculated variations in intensities averaged over multiple spectral measurements, the proposed method retained the statistical distribution of multiple independently determined plasma excitation temperatures. Therefore, this approach made it possible to directly evaluate the mean value, *SD*, *RSD*, and combined uncertainty of plasma excitation temperature, thus providing a physically meaningful estimate of the plasma excitation temperature with an associated statistical uncertainty. Finally, the presented methodology is promising for improving the accuracy of LIBS–based plasma–temperature determination that may be useful for improving plasma–temperature characterization in calibration–free LIBS applications.

5. ACKNOWLEDGEMENTS

We are grateful to the Pakistan Academy of Sciences for support to establish the LIBS setup at the National Centre for Physics, Islamabad.

6. CONFLICT OF INTEREST

The authors declare no conflict of interest.

7. ETHICAL STATEMENT

This study did not involve human participants or animals; therefore, ethical approval was not required.

8. FUNDING

No funding was received to conduct this research.

9. AUTHORSHIP CONTRIBUTION

Saba Munir: Writing original draft, Conceptualization, Methodology; **Nasar Ahmed**: Conceptualization, Analysis, Validation; **Amir Fayyaz**: Data acquisition and analysis, Conceptualization, Methodology; **Usman Liaqat**: Software, Conceptualization, Methodology; **Rinda Hedwig**: Software, Conceptualization, Validation; **M. Aslam Baig**: Supervision, Resources, Writing, reviewing and editing.

10. DECLARATION STATEMENT

We confirm that data presented here are the original results of authors, all authors have approved the manuscript, and if accepted for publication copyrights will be transferred to the Pakistan Academy of Sciences.

ACCEPTED MANUSCRIPT

11. REFERENCES

1. L.B. Guo, D. Zhang, L.X. Sun, S.C. Yao, L. Zhang, Z.Z. Wang, Q.Q. Wang, H.B. Ding, Y. Lu, Z.Y. Hou, and Z. Wang. Development in the application of laser-induced breakdown spectroscopy in recent years: A review. *Frontiers of Physics* 16(2): 22500 (2021). https://doi.org/10.1007/s11467-020-1007-z
2. D.W. Hahn and N. Omenetto. Laser-induced breakdown spectroscopy (LIBS), part II: review of instrumental and methodological approaches to material analysis and applications to different fields. *Applied spectroscopy* 66(4): 347-419 (2012). https://doi.org/10.1366/11-06574
3. M.K. Jean-Noël, K.T. Arthur, and B. Jean-Marc. LIBS technology and its application: overview of the different research areas. *Journal of Environmental Science and Public Health* 4(3): 134-149 (2020). https://doi.org/10.26502/jesph.96120090
4. W. Huang, C. Niu, K. Li, N. Deng, D. Zhang, Z. Hu, J. Zhang, and L. Guo. Recent advances in laser-induced breakdown spectroscopy instruments. *Frontiers of Physics* 21(7): 072202 (2026). https://doi.org/10.15302/frontphys.2026.072202
5. D.S. Ferreira, D.V. Babos, M.H. Lima-Filho, H.F. Castello, A.C. Olivieri, F.M. Verbi Pereira, and E.R. Pereira-Filho. Laser-induced breakdown spectroscopy (LIBS): calibration challenges, combination with other techniques, and spectral analysis using data science. *Journal of Analytical*

Atomic Spectrometry 39(12): 2949-2973 (2024). https://doi.org/10.1039/d4ja00250d

6. F. Zhao, X. Zhao, T. Jiang, R. Zhao, and F. Wu. Comprehensive study of CoCrCuNi high-entropy alloys: effects of preparation, heat treatment, computational simulation, and alloying elements. *Metals* 14(11): 1240 (2024). https://doi.org/10.3390/met14111240
7. F.J. Fortes, J. Moros, P. Lucena, L.M. Cabalín, and J.J. Laserna. Laser-induced breakdown spectroscopy. *Analytical chemistry* 85(2): 640-669 (2013). https://doi.org/10.1021/ac303220r
8. M.A. Ismail, H. Imam, A. Elhassan, W.T. Youniss, and M.A. Harith. LIBS limit of detection and plasma parameters of some elements in two different metallic matrices. *Journal of Analytical atomic Spectrometry* 19(4): 489-494 (2004). https://doi.org/10.1039/b315588a
9. V.K. Unnikrishnan, K. Alti, V.B. Kartha, C. Santhosh, G.P. Gupta, and B.M. Suri. Measurements of plasma temperature and electron density in laser-induced copper plasma by time-resolved spectroscopy of neutral atom and ion emissions. *Pramana* 74(6): 983–993 (2010). https://doi.org/10.1007/s12043-010-0089-5
10. N. Zhang, T. Ou, M. Wang, Z. Lin, C. Lv, Y. Qin, J. Li, H. Yang, N. Zhao, and Q. Zhang. A brief review of calibration-free laser-induced breakdown spectroscopy. *Frontiers in Physics* 10: 887171 (2022). https://doi.org/10.3389/fphy.2022.887171
11. E. Tognoni, G. Cristoforetti, S. Legnaioli, and V. Palleschi. Calibration-free laser-induced breakdown spectroscopy: state of the art. *Spectrochimica Acta Part B: Atomic Spectroscopy* 65(1): 1-14 (2010). https://doi.org/10.1016/j.sab.2009.11.006
12. A.M. Roldán, M. Pisarčík, M. Veis, M. Držík, and P. Veis. Calibration-free analysis of a tungsten-based target for diagnostics of relevant fusion materials comparing picosecond and nanosecond LIBS. *Spectrochimica Acta Part B: Atomic Spectroscopy* 177: 106055 (2021). https://doi.org/10.1016/j.sab.2020.106055
13. B. Bousquet, V. Gardette, V.M. Ros, R. Gaudiuso, M. Dell'Aglio, and A. De Giacomo. Plasma excitation temperature obtained with Boltzmann plot method: Significance, precision, trueness and accuracy. *Spectrochimica Acta Part B: Atomic Spectroscopy* 204: 106686 (2023). https://doi.org/10.1016/j.sab.2023.106686
14. L.M. John, R.C. Issac, S. Sankararaman, and K.K. Anoop. Multi-element Saha Boltzmann plot (MESBP) coupled calibration-free laser-induced breakdown spectroscopy (CF-LIBS): an efficient approach for quantitative elemental analysis. *Journal of Analytical Atomic Spectrometry* 37(11): 2451-2460 (2022). https://doi.org/10.1039/d2ja00218c
15. I.B. Gornushkin, S.V. Shabanov, S. Merk, E. Tognoni, and U. Panne. Effects of non-uniformity of laser induced plasma on plasma temperature and concentrations determined by the Boltzmann plot method: implications from plasma modeling. *Journal of Analytical Atomic Spectrometry* 25(10): 1643-1653 (2010). https://doi.org/10.1039/c0ja00016g
16. M.A. Baig, A. Fayyaz, R. Ahmed, Z.A. Umar, H. Asghar, U. Liaqat, R. Hedwig, and K.H. Kurniawan. Analytical techniques for elemental analysis: LIBS, LA-TOF-MS, EDX, PIXE, and XRF: A review. *Proceedings of the Pakistan Academy of Sciences: A. Physical and Computational Sciences* 61(2): 99-112 (2024). https://doi.org/10.53560/PPASA(61-2)676
17. A. Fayyaz, M. Waqas, H. Asghar, R. Ahmed, U. Liaqat, K. Naseem, and M.A. Baig. Rapid elemental imaging of copper-bearing critical ores using laser-induced breakdown spectroscopy coupled with PCA and PLS-DA. *Talanta* 296: 128463 (2026). https://doi.org/10.1016/j.talanta.2025.128463
18. M.A. Baig, A. Fayyaz, U. Liaqat, H. Asghar, and R. Ahmed. Signal Enhancement Techniques in LIBS-Based Experimentations. In: Laser Induced Breakdown Spectroscopy (LIBS): Chemometrics, Environmental and Forensic Applications. V.K. Singh (Ed.). *Springer Cham, Switzerland* pp. 143-183 (2025). https://doi.org/10.1007/978-3-031-90970-2_8
19. National Institute of Standards and Technology (NIST) Database. https://physics.nist.gov/PhysRefData/ASD/lines_form.html (accessed on 30 July 2026).
20. T.A. Alrebdi, A. Fayyaz, H. Asghar, A. Kamal, J. Iqbal, and N.K. Piracha. Chemometrics and spectroscopic analyses of peganum harmala plant's seeds by laser-induced breakdown spectroscopy. *Applied Sciences* 13(5): 2780 (2023). https://doi.org/10.3390/app13052780
21. D.A. Cremers and L.J. Radziemski (Eds.). Handbook of laser-induced breakdown spectroscopy. *John Wiley & Sons* (2013). https://doi.org/10.1002/9781118567371.index
22. A. Ciucci, M. Corsi, V. Palleschi, S. Rastelli, A. Salvetti, and E. Tognoni. New procedure for quantitative elemental analysis by laser-induced plasma spectroscopy. *Applied*

ACCEPTED MANUSCRIPT

spectroscopy 53(8): 960-964 (1999). https://doi.org/10.1366/0003702991947612

23. F. Poggialini, B. Campanella, B. Cocciaro, G. Lorenzetti, V. Palleschi, and S. Legnaioli. Catching up on calibration-free LIBS. *Journal of Analytical Atomic Spectrometry* 38(9): 1751-1771 (2023). https://doi.org/10.1039/d3ja00130j
24. J. Guezenoc, A. Gallet-Budynek, and B. Bousquet. Critical review and advices on spectral-based normalization methods for LIBS quantitative analysis. *Spectrochimica Acta Part B: Atomic Spectroscopy* 160: 105688 (2019). https://doi.org/10.1016/j.sab.2019.105688
25. J. Wang, M. Shi, P. Zheng, and S. Xue. Quantitative analysis of lead in tea samples by laser-induced breakdown spectroscopy. *Journal of Applied Spectroscopy* 84(1): 188-193 (2017). https://doi.org/10.1007/s10812-017-0448-9
26. U. Aydin, P. Roth, C.D. Gehlen, and R. Noll. Spectral line selection for time-resolved investigations of laser-induced plasmas by an iterative Boltzmann plot method. *Spectrochimica Acta Part B: Atomic Spectroscopy* 63(10): 1060-1065 (2008). https://doi.org/10.1016/j.sab.2008.08.003
27. A.S. Altowyan, A. El-Hussein, H.A. Ahmed, H.H. Faqih, A.S. Amein, A.M. Mostafa, and M.M. ElFaham. Influence of the laser wavelength on the self-absorption of Cu and Ni spectral lines by using LIBS technique. *Optical Materials* 131: 112731 (2022). https://doi.org/10.1016/j.optmat.2022.112731

ACCEPTED MANUSCRIPT